Eur Radiol (2013) 23:2814–2822
DOI 10.1007/s00330-013-2897-8

MUSCULOSKELETAL

Bi-exponential T2* analysis of healthy and diseased Achilles tendons: an in vivo preliminary magnetic resonance study and correlation with clinical score

Vladimir Juras · Sebastian Apprich · Pavol Szomolanyi · Oliver Bieri · Xeni Deligianni · Siegfried Trattnig

Received: 6 February 2013 / Revised: 9 April 2013 / Accepted: 15 April 2013 / Published online: 13 June 2013

Abstract
Objective To compare mono- and bi-exponential T_2* analysis in healthy and degenerated Achilles tendons using a recently introduced magnetic resonance variable-echo-time sequence (vTE) for T_2* mapping.
Methods Ten volunteers and ten patients were included in the study. A variable-echo-time sequence was used with 20 echo times. Images were post-processed with both techniques, mono- and bi-exponential [T_2*$_m$, short T_2* component (T_2*$_s$) and long T_2* component (T_2*$_l$)]. The number of mono- and bi-exponentially decaying pixels in each region of interest was expressed as a ratio (B/M). Patients were clinically assessed with the Achilles Tendon Rupture Score (ATRS), and these values were correlated with the T_2* values.
Results The means for both T_2*$_m$ and T_2*$_s$ were statistically significantly different between patients and volunteers; however, for T_2*$_s$, the *P* value was lower. In patients, the Pearson correlation coefficient between ATRS and T_2*s was −0.816 (P=0.007).
Conclusion The proposed variable-echo-time sequence can be successfully used as an alternative method to UTE sequences with some added benefits, such as a short imaging time along with relatively high resolution and minimised blurring artefacts, and minimised susceptibility artefacts and chemical shift artefacts. Bi-exponential T_2* calculation is superior to mono-exponential in terms of statistical significance for the diagnosis of Achilles tendinopathy.
Key Points
- *Magnetic resonance imaging offers new insight into healthy and diseased Achilles tendons*
- *Bi-exponential T2* calculation in Achilles tendons is more beneficial than mono-exponential*
- *A short T2* component correlates strongly with clinical score*
- *Variable echo time sequences successfully used instead of ultrashort echo time sequences*

Keywords Achilles tendon · Bi-exponential · T2* · ATRS · Mono-exponential · Magnetic resonance imaging

V. Juras (✉) · S. Apprich · P. Szomolanyi · S. Trattnig
Center of Excellence for High field MR, Department of Radiology, Medical University of Vienna, Waehringer Guertel 18-20, A-1090 Vienna, Austria
e-mail: vladimir.juras@meduniwien.ac.at

S. Apprich
e-mail: sebastian.apprich@meduniwien.ac.at

P. Szomolanyi
e-mail: pavol.szomolanyi@meduniwien.ac.at

S. Trattnig
e-mail: siegfried.trattnig@meduniwien.ac.at

V. Juras · P. Szomolanyi
Department of Imaging Methods, Institute of Measurement Science, Dubravska cesta 9, 84104 Bratislava, Slovakia

O. Bieri · X. Deligianni
Division of Radiological Physics, Department of Radiology, University of Basel Hospital, Basel, Switzerland

O. Bieri
e-mail: oliver.bieri@unibas.ch

X. Deligianni
e-mail: xeni.deligianni@unibas.ch

Introduction

It is generally known that biophysical properties of the tissue define the contrast between tissues in magnetic resonance imaging (MRI). In addition to field strength and temperature, relaxation times also depend on the macromolecular content

of the tissue. In highly organised tissues, such as tendons, ligaments, menisci, trabecular bone, or cartilage, the transversal relaxation time is extremely short compared with that of muscles or fat, for instance. Therefore, special MR sequences are required to acquire signal directly from these tissues. In the last 10 years, the most frequently used sequences for quantitative imaging of fast-relaxing tissues comprised the 3D ultrashort echo time (UTE) [1], the 2D-UTE [2], the stack of spirals (AWSOS) [3], and a variable echo time sequence [4, 5]. Macromolecular content causes strong anisotropy in these tissues through the dipole-dipole interaction. In the past, different degrees of anisotropy were observed in various tissues using spectroscopic methods; e.g. in tendons, four peaks were observed in the T_2 spectrum and in the cartilage two were observed [6, 7]. The recent developments in MR hardware and software now allow a quantification of multiple T_2 (or T_2*) components in the clinical environment. These can be subsequently used as markers for different pathophysiological conditions. In recently published studies, T_2* has been used as a marker for sub-clinical changes in menisci after an anterior cruciate ligament tear [8]. In other studies, osteoarthritis progression in cartilage was detected using T_2/T_2* [9–11]. As for tendons, several studies have demonstrated the suitability of quantitative T_2* mapping in the Achilles tendon [12, 13]. Generally, two types of water exist in connective tissues, free water and bound water, where the water molecules can be bound to collagen fibres or proteoglycan molecules. A common problem of bi-component T_2* analysis is that the shortest component is difficult to quantify with clinically common echo times (i.e. TE>10 ms). Another problem is a relatively high sensitivity to the signal-to-noise ratio (SNR) during multiple-component analysis. In our study, a 3D gradient echo (GRE) sequence with a variable echo time (vTE) was used. This sequence, which was introduced by Ying and Schmalbrock [5], and further developed by Song and Wehrli [4] and recently by Deligianni et al. [14], utilises varying phase-encoding gradients to manipulate the effective echo time, resulting in sub-millisecond TE that enables the visualisation of fast-relaxing tissues. The advantage of UTE sequences is the sampling of the MR signal with very short echo times, which allows T_2/T_2* to be calculated quite precisely. However, low resolution and blurring artefacts complicate T_2/T_2* estimation. The vTE offers images with high resolution without blurring. To the best of our knowledge, this sequence has not been previously used for T_2* calculation in the human Achilles tendon in vivo.

Therefore, the aim of this study was to confirm the suitability of vTE for T_2* estimation in the human Achilles tendon in vivo. Furthermore, we hypothesise that the echo time range provided by vTE would be suitable for bi-exponential T_2* calculation. We also compared the mono- and bi-exponentially calculated T_2* to demonstrate that the short and long T_2* components might help in diagnosing a degenerated Achilles tendon better than simple mono-exponentially calculated T_2*. To validate this, quantitative MRI data were correlated with clinical scores for Achilles tendon rupture.

Materials and methods

Patient cohort

Institutional Review Board approval and written, informed consent were obtained. Ten patients (mean age, 43.9± 13.4 years) with a painful Achilles tendon and ten age-matched, healthy volunteers (mean age, 43.7±11.2 years) were included in the study. The exclusion criteria for all subjects were contraindications to MR imaging.

MRI examination

All subjects were examined with a 3-T whole-body system (TIM Trio, Siemens, Erlangen, Germany) using an eight-channel knee coil (In Vivo, Gainesville, FL, USA). For quantitative bi-exponential T_2* assessment, a multi-echo, variable echo time (me-vTE) sequence was obtained, with sequentially shifted echo times. In total, there were five sets with four echo times each. There were 20 echo times: TE=0.8, 2.1, 3.1, 4.1, 5.1, 6.1, 7.1, 8.1, 9.1, 10.1, 11.1, 12.1, 13.1, 14.1, 15.1, 16.1, 17.1, 18.1, 19.1, and 20.0 ms. Other parameters were set as follows: field of view 118×180 mm, matrix 168×256, section/slice thickness 0.7 mm, 320 Hz/pixel bandwidth, and 144 sections, resulting in a total acquisition time of 12.16 min. For morphological evaluation of the Achilles tendon, the following set of four sequences was used: fat-saturated sagittal proton-density weighted turbo-spin echo (sag PD TSE), axial T_2-weighted TSE (ax T2 TSE), fat-saturated axial PD-weighted TSE (ax PD TSE), and a fat-saturated sagittal T_1-weighted sequence (sag T1). The parameters for these sequences are listed in Table 1.

Clinical tendon scoring

All subjects were rated according to the Achilles tendon Total Rupture Score (ATRS; 0–100 points, worst to best) [15]. The ATRS scoring sheet is summarised in Table 2. An orthopaedic surgeon with 5 years of experience (N.N.) rated the tendons.

Image analysis

Magnetic resonance imaging parameters were calculated using a manually drawn ROI analysis in the three regions of the Achilles tendon (insertion part, INS; middle part, MID; muscle-tendon junction, MTJ; Fig. 1). The length of each of the parts was defined as one-third of the total Achilles tendon

Table 1 Parameters for the sequences used for morphological evaluation of the Achilles tendon

	sag PD TSE	ax T2 TSE	ax PD TSE	sag T1
Orientation	Sagittal	Axial	Axial	Sagittal
TE [ms]	26	98	27	11
TR [ms]	3970	6720	3520	600
FOV read [mm]	220	170	170	220
PAT mode	GRAPPA	GRAPPA	GRAPPA	GRAPPA
Acceleration factor	2	2	2	2
Flip angle [°]	120	120	120	70
Averages	1	1	3	3
Slices	17	30	30	17
Slice thickness [mm]	2	4	4	2
Bandwidth [Hz/px]	149	177	149	160
Matrix	448×381	448×448	896×896	512×512
Total acq. time [min:s]	5:46	3:22	3:49	2:48

TE echo time, TR repetition time, PAT parallel acquisition techniques, GRAPPA generalised autocalibrating partially parallel acquisitions

length, measured from the most proximal to the most distal. Values were also stored for the sum of all three regions, hereafter referred to as the 'bulk' values. Images from the vTE sequence were analysed using a custom-written script in IDL 6.3 (Interactive Data Language, Research Systems, Inc., Boulder, CO, USA). A mono- as well as a bi-exponential fitting procedure was performed on all MR data sets on a pixel-by-pixel basis. For mono-exponential fitting, a three-parametric function was used to fit the signal intensity

$$S_m = A_0 * \exp\left(-TE \Big/ A_1\right) + A_2 \qquad ([1])$$

where A_0 is the signal intensity at a TE<1 ms, A_1 corresponds to the actual T_2*_m (mono-exponentially calculated T_2*), and A_2 is the baseline (mostly the noise). The same data set was also processed bi-exponentially, using the function

$$S_b = B_0 * \exp\left(-TE \Big/ B_1\right) + B_2 * \exp\left(-TE \Big/ B_3\right) + B_4 \qquad ([2])$$

where B_1 corresponds to the short component of T_2* (T_2*_s), B_3 corresponds to the long component of T_2* (T_2*_l), and B_0 and B_2 are the component ratios expressed further as a percentage value of B_0+B_2: $Fs=100*B_0/(B_0+B_2)$ and $F_l=100*B_2/(B_0+B_2)$. B_4 is the offset given primarily by noise.

Table 2 Achilles Tendon Total Rupture Score (ATRS) sheet (the numbers mean level of limitation) [15]

1. Are you limited because of decreased strength in the calf/Achilles tendon/foot?										
0	1	2	3	4	5	6	7	8	9	10
2. Are you limited because of fatigue in the calf/Achilles tendon/foot?										
0	1	2	3	4	5	6	7	8	9	10
3. Are you limited because of stiffness in the calf/Achilles tendon/foot?										
0	1	2	3	4	5	6	7	8	9	10
4. Are you limited because of pain in the calf/Achilles tendon/foot?										
0	1	2	3	4	5	6	7	8	9	10
5. Are you limited during activities of daily living?										
0	1	2	3	4	5	6	7	8	9	10
6. Are you limited when walking on uneven surfaces?										
0	1	2	3	4	5	6	7	8	9	10
7. Are you limited when walking quickly up the stairs or up a hill?										
0	1	2	3	4	5	6	7	8	9	10
8. Are you limited during activities that include running?										
0	1	2	3	4	5	6	7	8	9	10
9. Are you limited during activities that include jumping?										
0	1	2	3	4	5	6	7	8	9	10
10. Are you limited in performing hard physical labour?										
0	1	2	3	4	5	6	7	8	9	10

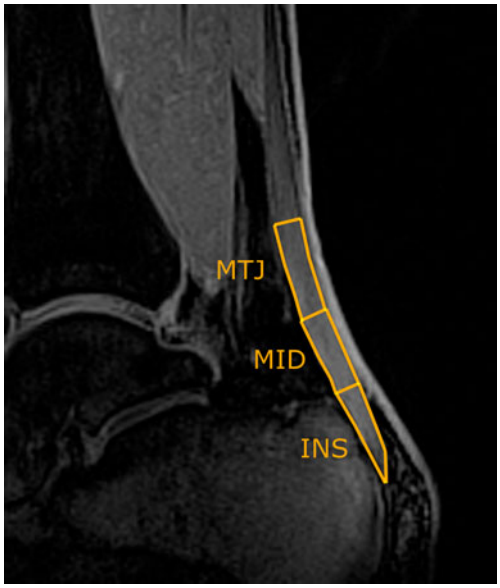

Fig. 1 Region-of-interest placement on vTE image (calculated as a subtraction of images acquired at TE=0.8 ms and TE=20 ms)

During the calculation of T_2*, only those pixels that satisfied the following condition were considered bi-exponential:

$$4 \times T_2{*}_s < T_2{*}_l \qquad ([3])$$

Seven maps for each slice were stored for further use, i.e. the mono-exponential T_2* maps, the short component of the bi-exponential T_2* maps, the long component of the bi-exponential T_2* maps, and both short and long T_2* component ratios and the binary maps of mono- or bi-exponentially calculated pixels. The map of the coefficient of determination (R^2, fit precision) and the binary map based on the bi-exponential condition (Eq.3) (0 = monoexponential decay, 1 = bi-exponential decay) were saved as well.

Each ROI was represented by a weighted mean value, calculated using an R^2 correction algorithm [16]. $T_2{*}_s$ and $T_2{*}_l$ were calculated using a mask created from a binary map, and only pixels that satisfied the condition $4 \times T_2{*}_s < T_2{*}_l$ were included. From each segment, the ratio of mono- and bi-exponential pixel amounts was calculated (further referred to as B/M).

Intra- and interobserver variation

To calculate the interobserver variability, all ten patients were evaluated by three independent raters (V.J., S.A., P.S.). The variation between raters was expressed as a coefficient of variation (CV, %). Intraobserver variability was calculated from three independent evaluations of ten patients by one rater (V.J.) and expressed as an intraclass correlation (ICC).

Statistical analysis

All statistical analyses were performed in SPSS for Windows, version 16.0 (SPSS Institute, Chicago, IL, USA). Descriptive statistics were performed in order to calculate the mean and standard deviation (SD) of age, $T_2{*}_m$, $T_2{*}_s$, $T_2{*}_l$, component ratios, B/M values, and ATRS separately for normal and degenerative Achilles tendons. An independent sample *t*-test with equal variances was performed to obtain the difference in individual parameters between the two groups. A P value<0.05 was considered statistically significant. The correlation of MR parameters and ATRS was calculated as a Pearson correlation coefficient. A binary classification test was performed on the data to obtain the discrimination power using ROC analyses. The area under the curve was calculated by using the trapezoidal rule and expressed as percentages.

Results

The coefficient of variation (CV) for interobserver variation was found to be 8.2 %, on average. For different tendon segments, the CV was 5.1 % for the insertion part of the tendon, 7.9 % for the mid part, and 11.8 % for the muscle-tendon junction. Intraobserver variation was expressed using ICC and found to be 0.881, on average. For different segments, ICC was 0.912 for the insertion part of the tendon, 0.845 for the mid part, and 0.887 for the muscle-tendon junction.

The mean ATRS was 52.8±23.7 for patients; all volunteers had an ATRS equal to 100. The mean pixel count for bulk ROIs was 307±134; separately, for the individual tendon parts, the INS was 106±48, the MID 114±54, and the MTJ 87±64. The model with the bi-exponential fitting function calculated the values with slightly higher precision than that with a mono-exponential fitting function (R^2[mono]=0.965±0.144; R^2[bi]=0.996±0.131). The data with the corresponding mono- and bi-exponential fits are depicted in Fig. 2. As for results from bulk analysis, in volunteers, the mean $T_2{*}_m$ was 3.35±0.45 ms, the mean $T_2{*}_s$ was 0.68±0.05 ms, the mean $T_2{*}_l$ was 16.99±7.11 ms, and the B/M ratio was 7.29±2.30. In patients, the mean $T_2{*}_m$ was 6.56±1.70 ms, the mean $T_2{*}_s$ was 0.87±0.08 ms, the mean $T_2{*}_l$ was 19.83±7.13 ms, and the B/M ratio was 3.39±1.27. The means for both $T_2{*}_m$ and $T_2{*}_s$ were statistically significantly different between the patients and volunteers; however, the P value for $T_2{*}_s$ was substantially lower ($P<0.001$) than that of $T_2{*}_m$ ($P=0.001$). Moreover, the amount of bi-exponentially decaying pixels decreased with pathology ($P=0.012$). All MR parameters, ratios, as well as P values are summarised in Table 3. The area under the curve was 0.669 for $T_2{*}_m$, 0.638 for $T_2{*}_s$, 0.580 for $T_2{*}_l$, and 0.643 for B/M. Examples of the maps from a volunteer and a patient are depicted in Figs. 3 and 4.

In patients, the Pearson correlation coefficient between ATRS and T_2*s was r=−0.846 (P=0.002). High correlation, albeit lower compared with T_2*$_s$, was also observed between ATRS and T_2*$_m$ (r=−0.786, P=0.007). ATRS did not correlate with T_2*$_l$ (r=−0.216, P=0.55) or B/M (r=−0.02, P=0.956) (Fig. 5).

Discussion

The results of this study suggest that the variable echo time sequence based on a gradient echo is suitable for bi-component analysis of T_2* in the human Achilles tendon in vivo. Mono-exponential calculation of T_2* provides a weighted mean value from different components of transversal relaxation. This may lead to an underestimation of T_2*, especially in diseased tendons. From a biochemical point of view, the short component of T_2* is related to bound water and the long component to free water [17]. This is due to the existence of distinct water compartments with different transverse relaxation times in highly organised biological tissues [18]. T_2 and T_2* in tendons have been studied previously using various methods, such as MR spectroscopy, a standard Carr Purcell Meiboom Gill (CPMG) sequence, 2D sequences, and 3D UTE sequences. Peto et al. studied different water compartments in the Achilles tendon ex vivo using MR spectroscopy [19]. They demonstrated four water components by measuring four T_2* components, 1.1, 6.0, 18.9, and 79.8 ms, with the component ratios of 56, 26, 15, and 3 %. T_2* is substantially dependent on temperature and orientation to the main magnetic field [19]. Henkelman et al. also demonstrated four-component T_2 decay in the Achilles tendon using a CMPG technique [6]. Despite this fact, there are many studies using mono-exponential T_2/T_2* calculations that have resulted in a linear combination of short and long T_2/T_2* components. Gold et al. used a projection-reconstruction approach to calculating T_2 in ex vivo Achilles tendons; the mean T_2 calculated in that study was 1.2±0.2 ms [20]. In another study, T_2* was calculated mono-exponentially using a 2D-UTE sequence in ex vivo samples [21], and it ranged from 1.76 to 2.64 ms for the global average area of the Achilles tendon. A bi-component analysis of transversal relaxation constants in the Achilles tendon is more sensitive to the precision of pixels used for fitting and is also more computationally demanding; however, it allows quantification of the bound and free water. The Graeme Bydder group performed the pioneer work in this field, mostly using 2D-UTE imaging and UTE spectroscopy imaging for fast-relaxing tissues [13, 17, 21, 22]. In a recent study by Diaz et al., investigators observed the different T_2* values in normal and abnormal Achilles tendons, with a short T_2* of 0.61±0.06 ms and a long T_2* of 8.23±1.29, and a short T_2* of 0.65±0.04 ms and a long T_2* of 4.72±0.77 ms in normal and abnormal tendons, respectively [23]. Du et al. described methods for bi-component analysis in a comprehensive study of bovine samples. They found two components of T_2* in the Achilles tendon (1.28±0.08 and 17.65±4.91 ms) and pointed out the importance of bi-component T_2* measurement in other tissues, such as ligaments, bone, meniscus, and even cartilage [17]. Robson et al. obtained regionally dependent T_2* values of 0.53 and 4.8 ms in the posterior part and 0.60 and 4.2 ms in the anterior part, and they observed a reduction in short T2 components in tendinopathy [13]. Juras et al. used 3D-UTE for bi-component calculation of T_2* and

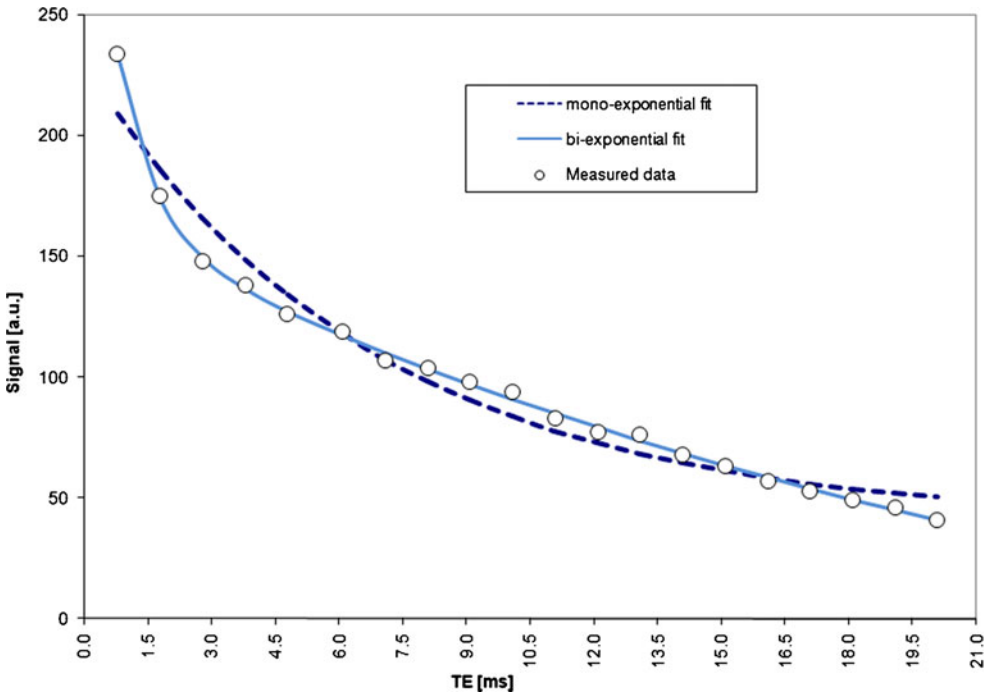

Fig. 2 Example of mono- and bi-exponential fit of data. The *solid line* represents the bi-exponential fit of the data, where T_2*$_s$ was 0.88 ms and T_2*$_l$ was 25.58 ms (with component ratios of 56 and 44 %, respectively). The *dashed line* represents the mono-exponential fit of the data, where T_2*$_m$ was 6.83 ms. R^2 was 0.9989 for the bi-exponential fit and 0.9120 for mono-exponential

Table 3 Summary of MR parameters in volunteers and patients, and statistical significance of the mean difference in different tendon structures

	Region	Volunteers		Patients		*P* values
		Mean	Standard deviation	Mean	Standard deviation	
T_2*_m	Bulk	3.35	0.45	6.56	1.70	0.001*
	INS	3.45	0.49	5.32	0.77	0.049*
	MID	4.42	1.16	8.91	1.88	0.033*
	MTJ	2.17	0.39	5.47	1.51	0.021*
T_2*_s	Bulk	0.68	0.05	0.87	0.08	<0.001*
	INS	0.68	0.05	0.95	0.16	0.006*
	MID	0.78	0.29	0.97	0.13	0.097
	MTJ	0.58	0.17	0.67	0.13	0.183
T_2*_l	Bulk	16.99	7.11	19.83	7.13	0.538
	INS	13.49	3.80	16.87	6.47	0.264
	MID	17.37	3.10	23.41	6.21	0.279
	MTJ	20.13	5.21	19.21	7.67	0.082
Short component	Bulk	58	10	60	9	2.150
	INS	56	11	61	8	0.259
	MID	56	11	61	9	0.144
	MTJ	57	12	62	6	0.078
Long component	Bulk	42	11	40	9	2.150
	INS	39	8	39	7	0.259
	MID	44	11	39	9	0.144
	MTJ	43	12	38	6	0.078
B/M	Bulk	7.29	2.30	3.39	1.27	0.012*
	INS	4.26	1.91	2.62	1.73	0.291
	MID	7.96	2.89	2.64	1.29	0.157
	MTJ	9.67	2.61	4.92	2.24	0.04*

Asterisk indicates statistical significance ($P<0.05$)

found significant differences between normal and degenerated Achilles tendons (0.34±0.09 and 10.28±2.28 ms versus 0.71 ±0.17, and 12.85±1.87 ms) [12]. Those authors found a significant increase in the short T_2* component in degenerative tendon tissue. However, these numbers were measured at 7 T; therefore, they may differ from those measured in this study at 3 T. Noticeably, the variation in the long T_2* component among the studies is much greater than that of the short component, which can provide an explanation for the lower clinical specificity and sensitivity of T_2*_l.

Interestingly, when comparing the T_2*_m and T_2*_s from the whole tendon between volunteers and patients, both

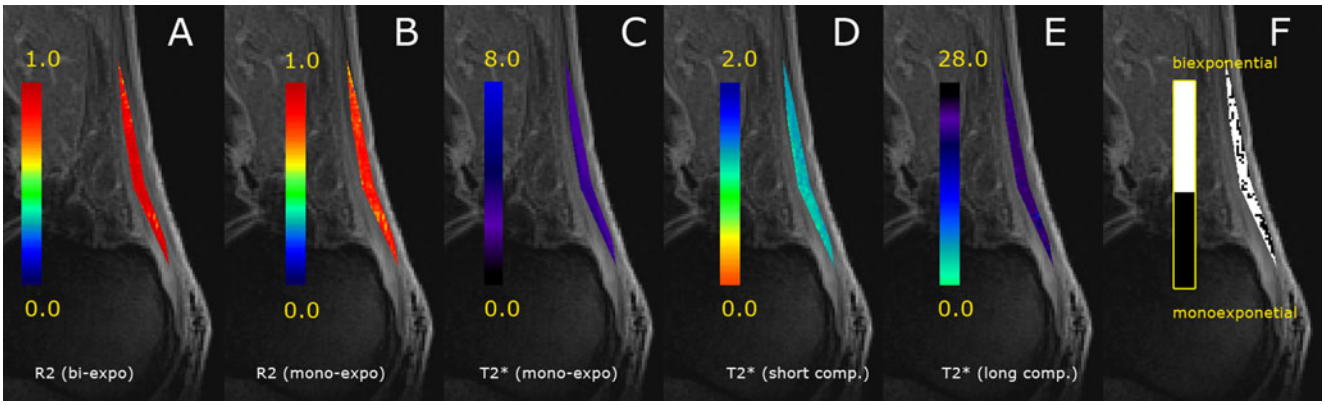

Fig. 3 Example of bi-component T_2* analysis of a 23-year-old healthy volunteer. **a** R^2 map for bi-exponential T_2* calculation; **b** R^2 map for mono-exponential T_2* calculation; **c** mono-exponentially calculated T_2*; **d** short component of T_2* map; **e** long component of T_2* map; **f** the binary map of mono- and- bi-exponential pixels used for B/M ratio calculation. Individual maps are overlaid on vTE images, calculated as a subtraction of the shortest TE (0.8 ms) and the longest TE (20 ms). Note the higher R^2 values for bi-exponential calculation

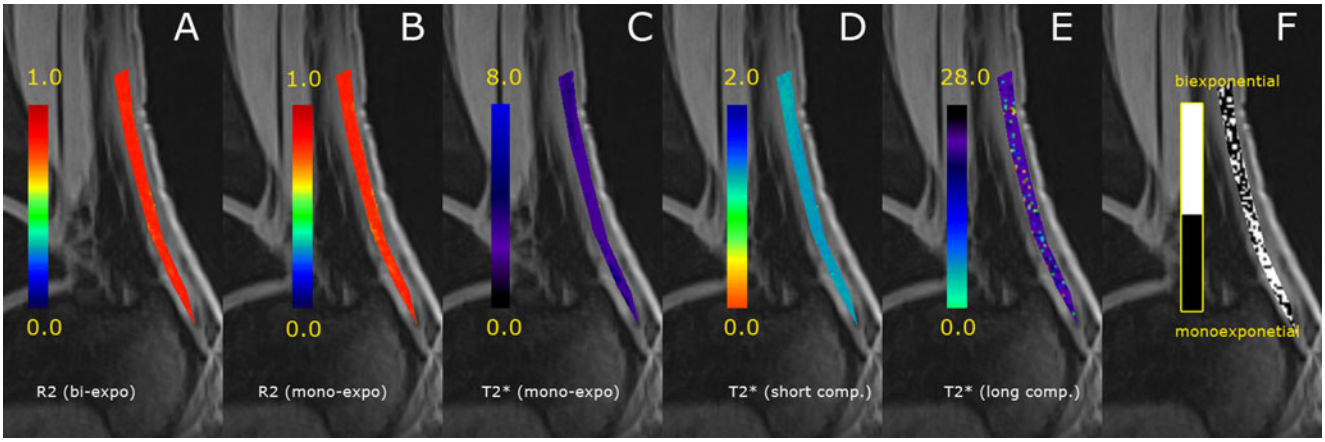

Fig. 4 Example of bi-component T_2* analysis of a 64-year-old patient with an ATRS of 45. **a** R^2 map for bi-exponential T_2* calculation; **b** R^2 map for mono-exponential T_2* calculation; **c** mono-exponentially calculated T_2*; **d** short component of T_2* map; **e** long component of T_2* map; **f** the binary map of mono- and- bi-exponential pixels used for B/M ratio calculation. Individual maps are overlaid on vTE images, calculated as a subtraction of the shortest TE (0.8 ms) and the longest TE (20 ms). Note the higher diversity of the long T_2* component and bi-exponential pixels, as well as the altered ratio of mono- and bi-exponentially calculated pixels compared to volunteer's data

mean differences were statistically significant. However, when looking at the separately segmented regions (INS, MID, and MTJ), the difference in T_2*$_m$ was statistically significant in all parts, while the difference in T_2*$_s$ was significant only in the insertion part. This can be explained by the fact that collagen fibre organisation is higher from the MTJ toward the INS; therefore, more pixels were excluded from bi-exponential analysis from the MTJ and MID parts of the tendon, which could have affected the statistics.

To the best of our knowledge, quantitative MRI values have not been correlated with the clinical scores, to date. The ATRS score has high clinical utility, being both patient- and clinician-friendly, and it has been validated in many studies [15, 24–26]. Although it was originally developed for measuring outcome after the treatment of total Achilles tendon rupture, it is also extendable to the general evaluation of the Achilles tendon status. The high correlation of T_2*m and T_2*s with clinical scores in our study validates the clinical value of quantitative MRI for Achilles tendons.

The intra- and interobserver variability showed a very high reproducibility for the evaluation. The highest variability was found in the MTJ part of the tendon, which is probably attributable to the more difficult segmentation in the region where the tendon connects to the soleus and gastrocnemius muscles.

Our study has several limitations. Possible patient movement may have introduced an error in the sensitive bi-exponential T_2*. Movement of the subjects was minimised by careful ankle fixation, and the images were also co-registered in the post-processing phase.

Some bias may have also been introduced by choosing the constant in the condition for bi-exponentially decaying pixels, which was based purely on empirical findings. This choice seemed to best fit the mathematical model of bi-exponential

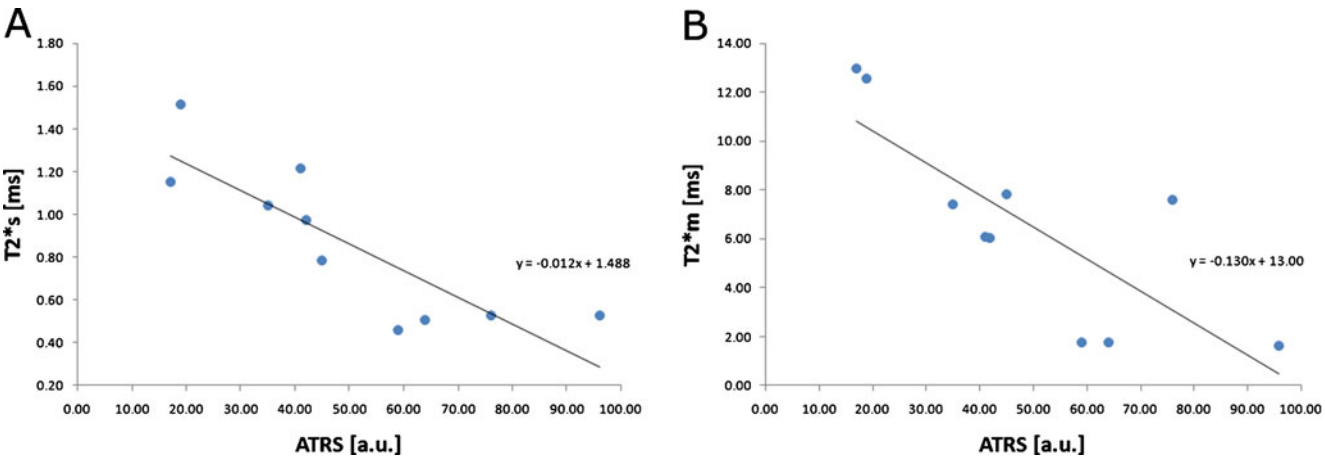

Fig. 5 **a** A scatter plot of the T_2*$_s$ and ATRS of ten patients. The Pearson correlation coefficient was r=−0.846 (P=0.002). **b** A scatter plot of the T_2*$_m$ and ATRS of ten patients. The Pearson correlation coefficient was r=−0.786 (P=0.007)

fitting at the noise level measured in this study; however, no detailed simulations were performed to validate this.

The magic angle effect may bring unwanted error to T_2/T_2* calculations. It has been shown that T_2* is approximately five times higher at 55° than at 0° for tendons and two times higher for entheses [22, 27]. To minimise this problem, we positioned our patients for MR imaging such that the Achilles tendon was in a direction parallel to B_0, and we tried to maintain the flexion of the ankle joint at 90°.

As the data in this study are presented as preliminary, further investigation with a larger patient cohort is necessary to validate the results.

The echo time range can be considered another limitation. The short T_2* component was sampled with the first two or three echo times, which may have introduced a greater uncertainty for the short component calculation, compared with the long component. However, the substantially higher precision (higher R^2) of the fitting curves suggests that bi-component analysis is valid. The robustness of the method may be further improved by increasing SNR via transferring to an ultra-high-field MR device.

This new method allows better definition of the different components of the collagen fibre network within the Achilles tendon, mainly the differentiation between the slow and fast component of the T_2* decay, which corresponds to the free and bound proton pool within this tissue. Thus, the detection of subtle abnormalities within the Achilles tendon seems to be feasible, and the high correlation with the clinical Achilles tendon score underlines its potential as a marker for different stages of Achilles tendon disease. The ability to obtain a higher intrastructural tendon analysis may also help to define Achilles tendinopathy that is at risk for a partial tear. Finally, this technique may help in the monitoring of Achilles tendon healing after full tear surgical treatment, as it provides the opportunity to detect earlier changes as a result of abnormal healing with the risk of a re-tear of the Achilles tendon

In conclusion, the vTE is a suitable sequence for T_2* mapping in the human Achilles tendon in vivo, and the echo range provided by this sequence (minimum echo time, 0.8 ms) is capable of two-component T_2* analysis. This sequence can be successfully used as an alternative to 2D and 3D UTE sequences with several benefits, such as a short imaging time, along with relatively high resolution and minimised blurring artefacts. The short component of T_2* provides a better marker of Achilles tendinopathy, suggesting that it reflects the changes in water content and collagen orientation more accurately than a simple mono-exponential fit.

Acknowledgement Funding support provided by the Austrian Science Fund (FWF) P 25246 B24, the Vienna Advanced Imaging Center (VIACLIC), and the Slovak Scientific Grant Agency VEGA, grant no. 2/0090/11.

References

1. Nielles-Vallespin S, Weber MA, Bock M et al (2007) 3D radial projection technique with ultrashort echo times for sodium MRI: Clinical applications in human brain and skeletal muscle. Magn Reson Med 57:74–81
2. Robson MD, Gatehouse PD, Bydder M, Bydder GM (2003) Magnetic resonance: An introduction to ultrashort TE (UTE) imaging. J Comput Assist Tomogr 27:825–846
3. Qian YX, Boada FE (2008) Acquisition-weighted stack of spirals for fast high-resolution three-dimensional ultra-short echo time MR imaging. Magn Reson Med 60:135–145
4. Song HK, Wehrli FW (1998) Variable TE gradient and spin echo sequences for in vivo MR microscopy of short T-2 species. Magn Reson Med 39:251–258
5. Ying K, Schmalbrock P, Clymer B (1995) Echo-time reduction for submillimeter resolution imaging with a 3D phase encode time reduced acquisition method. Magn Reson Med 33:82–87
6. Henkelman RM, Stanisz GJ, Kim JK, Bronskill MJ (1994) Anisotropy of NMR properties of tissues. Magn Reson Med 32:592–601
7. Zheng S, Xia Y (2009) Multi-components of T2 relaxation in ex vivo cartilage and tendon. J Magn Reson 198:188–196
8. Williams A, Qian Y, Golla S, Chu CR (2012) UTE-T2 * mapping detects sub-clinical meniscus injury after anterior cruciate ligament tear. Osteoarthr Cartil/OARS Osteoarthritis Res Soc 20:486–494
9. Taylor C, Carballido-Gamio J, Majumdar S, Li X (2009) Comparison of quantitative imaging of cartilage for osteoarthritis: T2, T1rho, dGEMRIC and contrast-enhanced computed tomography. Magn Reson Imaging 27(6):779–784
10. Welsch GH, Mamisch TC, Hughes T et al (2008) In vivo biochemical 7.0 Tesla magnetic resonance: preliminary results of dGEMRIC, zonal T2, and T2* mapping of articular cartilage. Investig Radiol 43:619–626
11. Mamisch TC, Hughes T, Mosher TJ et al (2012) T2 star relaxation times for assessment of articular cartilage at 3 T: a feasibility study. Skeletal Radiol 41:287–292
12. Juras V, Zbyn S, Pressl C et al (2012) Regional variations of T-2* in healthy and pathologic Achilles tendon in vivo at 7 Tesla: Preliminary results. Magn Reson Med 68:1607–1613
13. Robson MD, Benjamin M, Gishen P, Bydder GM (2004) Magnetic resonance imaging of the Achilles tendon using ultrashort TE (UTE) pulse sequences. Clin Radiol 59:727–735
14. Deligianni X, Bär P, Scheffler K, Trattnig S, Bieri O (2012) High-resolution Fourier-encoded sub-millisecond echo time musculoskeletal imaging at 3 Tesla and 7 Tesla. Magn Reson Med. doi:10.1002/mrm.24578 [Epub ahead of print]
15. Nilsson-Helander K, Thomee R, Gravare-Silbernagel K et al (2007) The Achilles Tendon Total Rupture Score (ATRS)—Development and validation. Am J Sports Med 35:421–426
16. Juras V, Zbyn S, Szomolanyi P, Trattnig S (2011) Regression error estimation significantly improves the region-of-interest statistics of noisy MR images. Med Phys 37:2813–2821
17. Du J, Diaz E, Carl M, Bae W, Chung CB, Bydder GM (2012) Ultrashort echo time imaging with bicomponent analysis. Magn Reson Med 67:645–649
18. Cameron IL, Short NJ, Fullerton GD (2007) Verification of simple hydration/dehydration methods to characterize multiple

water compartments on tendon type 1 collagen. Cell Biol Int 31:531–539
19. Peto S, Gillis P, Henri VP (1990) Structure and dynamics of water in tendon from NMR relaxation measurements. Biophys J 57:71–84
20. Gold G, Wren T, Nayak K, Nishimura D, Beaupre G (2001) In vivo short echo time imaging of Achilles tendon. Proc Intl Soc Mag Reson Med 9:244
21. Filho GH, Du J, Pak BC et al (2009) Quantitative characterization of the Achilles tendon in cadaveric specimens: T1 and T2* measurements using ultrashort-TE MRI at 3 T. Am J Roentgenol 192: W117–W124
22. Du J, Chiang AJT, Chung CB et al (2010) Orientational analysis of the Achilles tendon and enthesis using an ultrashort echo time spectroscopic imaging sequence. Magn Reson Imaging 28:178–184
23. Diaz E, Chung CB, Bae WC et al (2012) Ultrashort echo time spectroscopic imaging (UTESI): an efficient method for quantifying bound and free water. NMR Biomed 25:161–168
24. Lapidus LJ, Ray BA, Hamberg P (2012) Medial Achilles tendon island flap-a novel technique to treat reruptures and neglected ruptures of the Achilles tendon. Int Orthop 36:1629–1634
25. Kearney RS, Achten J, Lamb SE, Plant C, Costa ML (2012) A systematic review of patient-reported outcome measures used to assess Achilles tendon rupture management: What's being used and should we be using it? Br J Sports Med 46:1102–1109
26. Silbernagel KG, Steele R, Manal K (2012) Deficits in heel-rise height and Achilles tendon elongation occur in patients recovering from an Achilles tendon rupture. Am J Sports Med 40:1564–1571
27. Du J, Pak BC, Znamirowski R et al (2009) Magic angle effect in magnetic resonance imaging of the Achilles tendon and enthesis. Magn Reson Imaging 27:557–564